

Magnetic-Doublet Theory in the Analysis of Total-Intensity Anomalies

GEOLOGICAL SURVEY BULLETIN 1052-D



Magnetic-Doublet Theory in the Analysis of Total-Intensity Anomalies

By ROLAND G. HENDERSON and ISIDORE ZIETZ

EXPERIMENTAL AND THEORETICAL GEOPHYSICS

GEOLOGICAL SURVEY BULLETIN 1052-D

Discusses typical magnetic-doublet profiles and their use in the interpretation of aeromagnetic maps



UNITED STATES DEPARTMENT OF THE INTERIOR

FRED A. SEATON, *Secretary*

GEOLOGICAL SURVEY

Thomas B. Nolan, *Director*

CONTENTS

	Page
Abstract.....	159
Introduction.....	159
Limitations of magnetic interpretations.....	159
Fundamentals of depth estimation.....	160
Purpose and scope of investigation.....	160
Acknowledgments.....	161
Theoretical doublet anomalies.....	161
Formulation of interpretation factors.....	161
Analysis of anomalies.....	172
Other uses of computed anomalies.....	173
Magnetic model experiments.....	174
Tests on cylindrical models.....	174
Magnetic double-layer models.....	176
Practical applications.....	179
Southeast Missouri.....	179
Indiana.....	181
Ontario, Canada.....	183
Adirondack Mountains, N. Y.....	184
Conclusions.....	185
Literature cited.....	185

ILLUSTRATIONS

	Page
FIGURE 27. Total-intensity anomaly of inclined doublet; coordinate system and meaning of β and δ	162
28. Total-intensity anomalies of magnetic doublet of length, $l=0.01$ depth unit.....	163
29. Total-intensity anomalies of magnetic doublet of length, $l=0.1$ depth unit.....	164
30. Total-intensity anomalies of magnetic doublet of length, $l=0.5$ depth unit.....	165
31. Total-intensity anomalies of magnetic doublet of length, $l=1.0$ depth unit.....	165
32. Total-intensity anomalies of magnetic doublet of length, $l=1.5$ depth units.....	166
33. Total-intensity anomalies of magnetic doublet of length, $l=2$ depth units.....	167
34. Total-intensity anomalies of magnetic doublet of length, $l=5$ depth units.....	168
35. Total-intensity anomalies of doublets showing effect of increasing length, l	169
36. Total-intensity anomaly of inclined cylinder; obtained from model experiment.....	172

	Page
FIGURE 37. Total-intensity anomaly of magnetized plate; obtained from model experiment.....	176
38. Anomalies of inclined cylinders showing effect of increasing diameter.....	178
39. Total-intensity aeromagnetic map of part of Coldwater quadrangle, Missouri.....	180
40. Total-intensity aeromagnetic map of area near Bryant, Jay County, Ind.....	181
41. Total-intensity aeromagnetic map of T. 34 N., R. 3 W., La Porte County, Ind.....	182
42. Total-intensity aeromagnetic map of area near Marmora, Ontario, Canada.....	183
43. Total-intensity aeromagnetic map of northern part of Stark quadrangle, New York.....	184

TABLES

	Page
TABLE 1. Comparison of numerical values for two different definitions of β	166
2. Parameters of magnetic doublets for inclinations, I , and length-to-depth ratios, l/d	170
3. Comparison of calculated doublet lengths and depths with those used in model experiments.....	175
4. Application of magnetic-doublet theory to field of horizontal slab.....	177

EXPERIMENTAL AND THEORETICAL GEOPHYSICS

MAGNETIC-DOUBLET THEORY IN THE ANALYSIS OF TOTAL-INTENSITY ANOMALIES

By ROLAND G. HENDERSON and ISIDORE ZIETZ

ABSTRACT

Analysis of horizontal- or vertical-intensity magnetic anomalies in terms of equivalent magnetic doublets has been extensively used for rough estimates of depth and depth extent of disturbing rocks. In this investigation, factors have been theoretically determined by which appropriate total-intensity anomalies can also be analyzed in terms of their magnetic-doublet equivalents. The effectiveness and limitations of the method have been checked by application to anomalies derived from model experiments and to observed anomalies. For satisfactory results the effective radius of the disturbing body must be less than its depth of burial. The calculation of doublet length is not so reliable as the calculation of depth; however, the former is better at low magnetic latitudes.

INTRODUCTION

LIMITATIONS OF MAGNETIC INTERPRETATIONS

■ The results of aeromagnetic surveys are usually presented in the form of contour maps showing lines of equal total magnetic intensity. The anomalies of interest to exploration geophysicists are departures from smooth regularity, for they are indicative of inhomogeneities in the magnetism of the earth's crust. The relation of anomalies to subsurface geologic structure and to ore bodies is usually uncertain. For this reason interpretations of magnetic anomalies are often qualitative in nature, the map being discussed in terms of "grain" of the anomalies and generalization about likely contrasts in magnetic properties of the basement rocks from which the anomalies probably arise. In general, broad magnetic gradients several tens of miles in linear section represent regional variations in magnetization of the crust; anomalies 10 or 20 miles in lateral extent are associated with more abrupt changes in the magnetic character of the basement rocks; and areally small, high-gradient anomalies are indicative of near-surface concentrations of ferromagnetic materials.

[The quantitative interpretation of aeromagnetic maps is at once a complicated and challenging area of geophysical investigation. The complications stem largely from the presence of induced and permanent (sometimes called remanent) magnetism in the disturbing body, from lack of knowledge of the magnetic and geometric parameters of the body, and from an inherent ambiguity affecting interpretation of potential fields. The ambiguity arises from the fact that there are many distributions of magnetic material at various depths which can produce a given anomaly. Supplementary geological and geophysical information is therefore necessary for unequivocal solutions.

FUNDAMENTALS OF DEPTH ESTIMATION

Useful estimates of depths to disturbing bodies are often possible from magnetic anomalies despite these limitations. The relative positions of the maximums, minimums, and inflection points of an anomaly (the so-called shape factors) are functions of the depth and are affected only in a limited way by the remaining geometric parameters of the configuration of the body. These characteristic shape factors are unaffected by blockwise lateral changes in magnetic susceptibility of the basement or by the magnitude of the remanent magnetism when the latter is in the direction of the induced magnetism. Most methods of estimating depth are based on quasi-empirical facts deduced from studies of the shape characteristics of theoretical anomalies. Induction theory is used almost exclusively. It is assumed that the magnetization is the product of the susceptibility contrast and the normal field strength, and that the direction of magnetization is that of the normal field.

Since the advent of the airborne magnetometer, there have been several papers on methods of depth analysis. In the method outlined by Vacquier and others (1951), the shape characteristics of an observed field are compared with those of prismatic-model fields, the comparison being facilitated by the use of second derivatives of the anomaly which bring the shape characteristics into sharper focus. The method has been used successfully in depth analyses of many broad, large-amplitude anomalies (Zietz and Henderson, 1956; Henderson and Zietz, 1958).

PURPOSE AND SCOPE OF INVESTIGATION

Where the breadth of the anomaly is comparable to the depth of the source, the Vacquier method is less effective because the shape characteristics become more sensitive to parameters of the geometry other than the depth. Analyses of such anomalies can be made in terms of equivalent magnetic doublets. By equivalent magnetic doublet we mean two magnetic poles of equal strength and opposite

sign, whose depths below the surface and mutual displacement in the direction of the earth's normal field are sufficient to account for the shape characteristics of the anomaly. In standard texts on geophysics, such as Heiland (1940), Jakosky (1950), and Nettleton (1940), magnetic doublets are discussed in relation to the anomaly in the vertical component (ΔZ) and the anomaly in the horizontal component (ΔH), but no general treatment for depth calculations is given. Vestine and Davids (1945) presented an ingenious method for analyzing ΔZ in terms of magnetic doublets.

In airborne magnetometry, however, we are interested in the component of the total-intensity anomaly in the direction of the total field vector. It is a linear combination of ΔZ and ΔH and existing theory of the interpretation of doublets is not in general applicable. The work reported here was undertaken to establish a set of model anomaly curves for ΔT doublets and to deduce from them factors that are diagnostic of the doublet parameters. Major interest is centered in the calculation of depth to the upper (or nearer) pole; however, the more intractable problem of doublet length is also considered. There is some latitude in the choice of specific portions of an anomaly profile for formulating the factors. In every case the choice was dictated by considerations of usefulness in practical applications. The method has been tested by application to laboratory magnetic models, and its application to practical anomalies is demonstrated.

ACKNOWLEDGMENTS

We acknowledge our indebtedness to Mr. L. R. Alldredge, formerly of the Electricity and Magnetism Division of the Physics Research Department of the Naval Ordnance Laboratory, for the use of the magnetic testing equipment, and to Messrs. C. L. Parsons and K. E. Dornstreich, also of the Naval Ordnance Laboratory, for valuable technical assistance.

THEORETICAL DOUBLET ANOMALIES FORMULATION OF INTERPRETATION FACTORS

In this study it is tacitly assumed that the doublet is produced only by induction in the earth's magnetic field, and that the north dip of the doublet is equal to the magnetic inclination. A right-handed system of coordinates is adopted (fig. 27) with origin at O , x positive to magnetic north, y positive to the east, and z positive vertically downwards. The components of the magnetic field, ΔX , ΔY , and ΔZ , are positive along the respective coordinate axes. The doublet of strength m and length l lies in the xz plane; the coordinates of the pole nearer the origin are $(0, 0, d)$, and those of the remote pole are $(l \cos I, 0, d + l \sin I)$.

$$\Delta T(x) = \left\{ \frac{(x-l \cos I)}{[(l \cos I - x)^2 + (1+l \sin I)^2]^{3/2}} - \frac{x}{[x^2+1]^{3/2}} \right\} \cos I + \left\{ \frac{1}{[x^2+1]^{3/2}} - \frac{1+l \sin I}{[(l \cos I - x)^2 + (1+l \sin I)^2]^{3/2}} \right\} \sin I \quad (1)$$

From formula (1), $\Delta T(x)$ was computed for doublets with parameters $l/d=0.01, 0.10, 0.50, 1.00, 1.50, 2.00, 5.00$; and inclinations, $I=0^\circ, 30^\circ, 45^\circ, 60^\circ, 75^\circ, 90^\circ$. These are shown in figures 28 to 34.

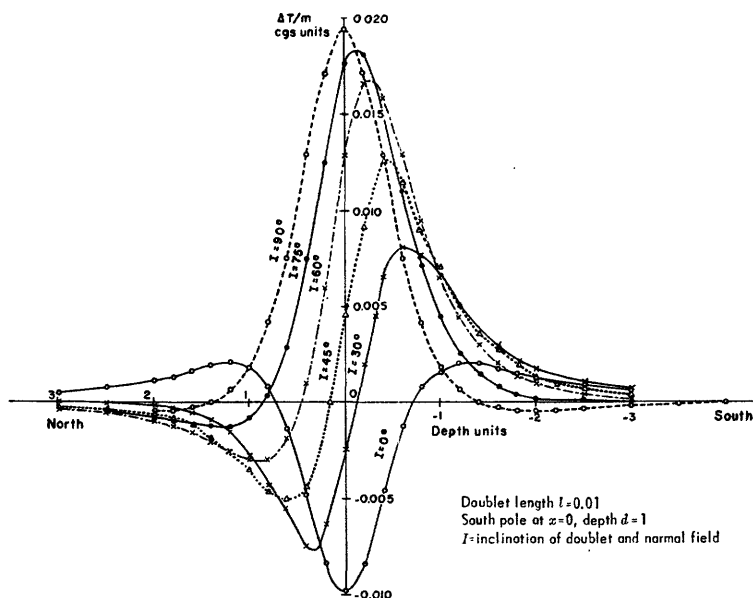


FIGURE 28.—Total-intensity anomalies of magnetic doublet of length, $l=0.01$ depth unit.

From an empirical study of theoretical doublet-anomaly curves of this type, it is possible to determine factors, herein designated β and δ , which are useful in estimating l and d from observed anomalies. The dimensionless factor β involves the ratio between certain horizontal distances subtended by the curve, and δ is a horizontal distance, usually between half-maximum abscissas or between nearly inflectional points. In figure 27, $\beta = (x'_{0.1} - x_{\max}) / (x_{\max} - x_{0.8})$ and $\delta = x'_{0.5} - x_{0.5}$ where x_{\max} , $x_{0.1}$, $x_{0.5}$, $x_{0.8}$ are the abscissas of ΔT_{\max} , $0.1 \Delta T_{\max}$, $0.5 \Delta T_{\max}$, and $0.8 \Delta T_{\max}$, respectively. Prime marks refer to the more northerly of two points.

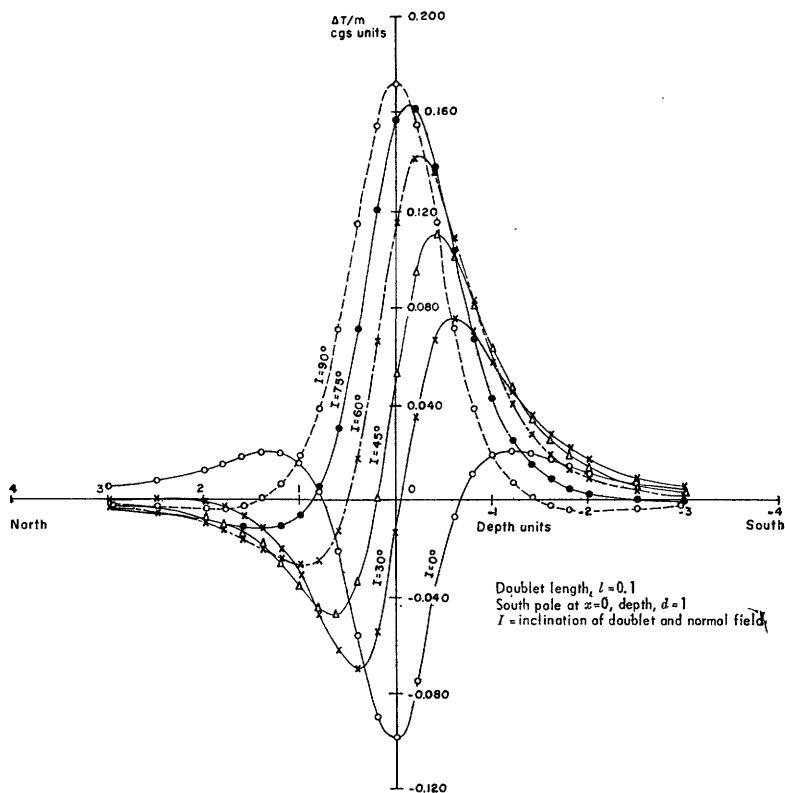
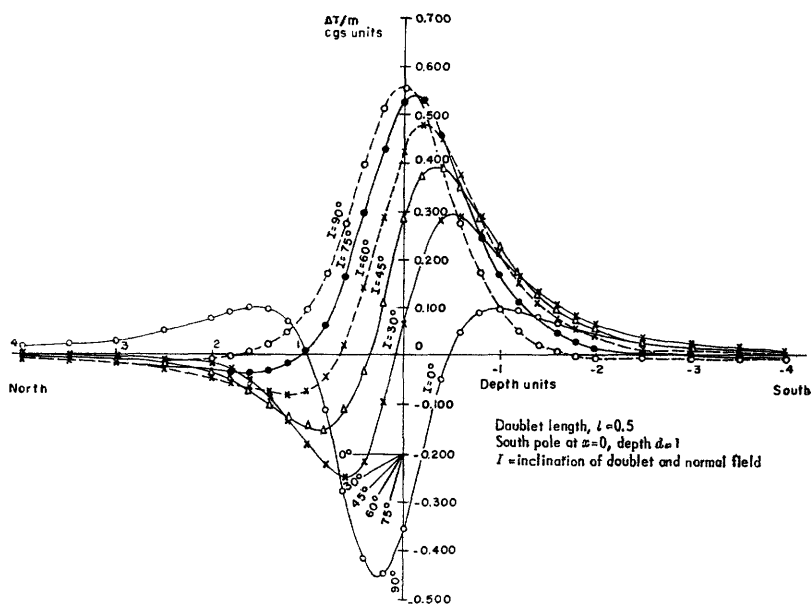
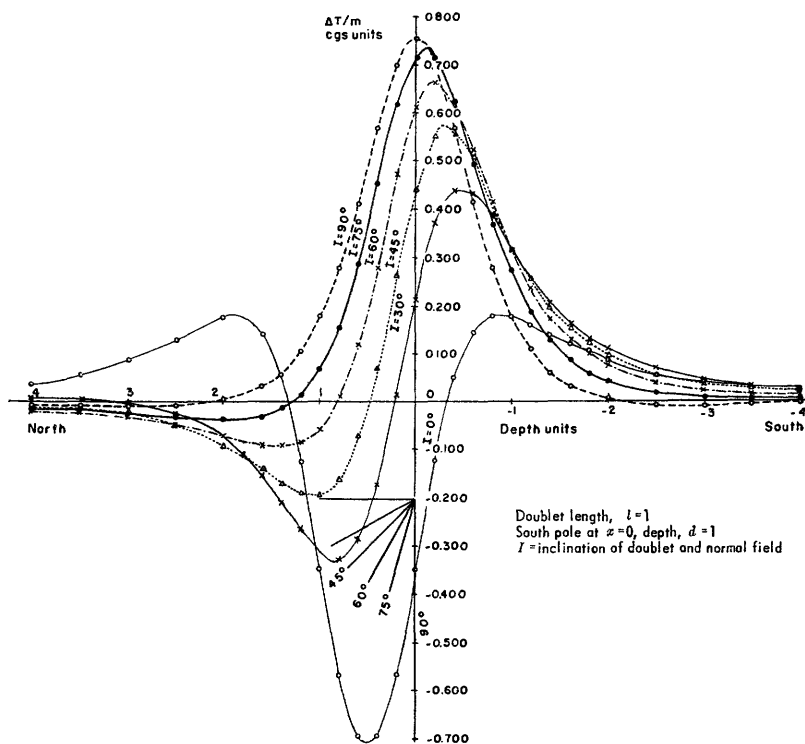


FIGURE 29.—Total-intensity anomalies of magnetic doublet of length, $l=0.1$ depth unit.

Practical considerations require that β be determined from portions of the curve that are easily identifiable and, at most, only slightly affected by nearby disturbances. Peripheral features should be avoided as far as possible. Moreover, β and δ must be so chosen that there will be resolution between successive values of l/d . To satisfy these requirements, β and δ are necessarily different for each inclination. The selection of abscissas is facilitated if the vertical scale of each of the family of $\Delta T(x)$ curves is adjusted so that all maximums have the same amplitude, as is shown in figure 35 for $I=75^\circ$. If in this figure, β were chosen in two different ways, say $\beta_1 = (x_{0.5} - x_{\max}) / (x_{\max} - x'_{0.5})$ and $\beta_2 = (x'_{0.1} - x_{\max}) / (x_{\max} - x_{0.8})$, the tabulation would be that shown in table 1.

FIGURE 30.—Total-intensity anomalies of magnetic doublet of length, $l=0.5$ depth unit.FIGURE 31.—Total-intensity anomalies of magnetic doublet of length, $l=1.0$ depth unit.

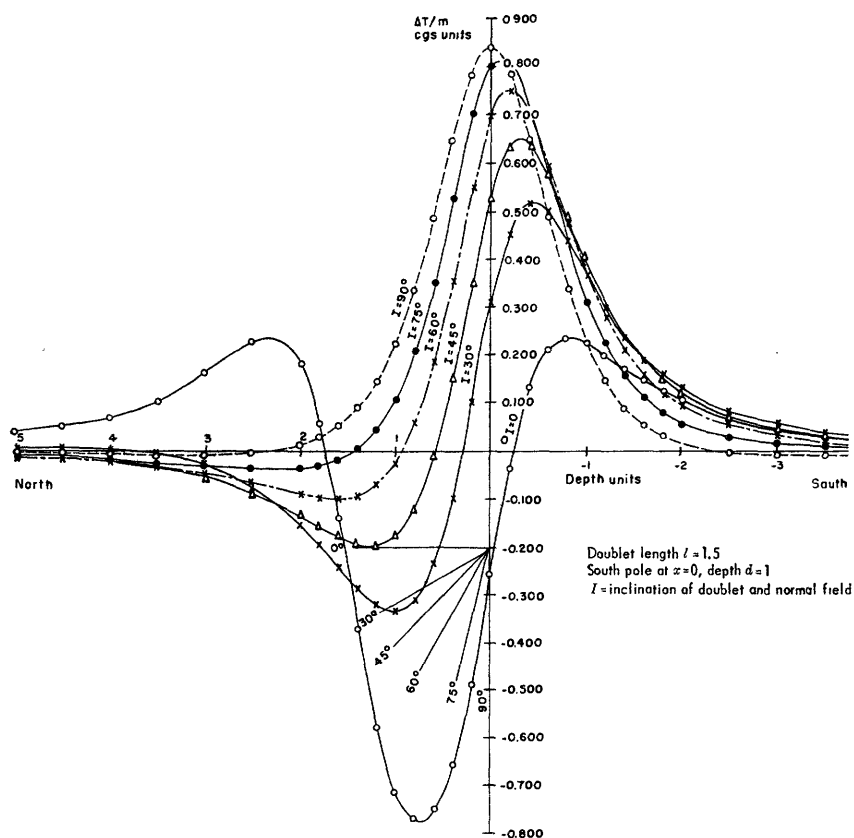


FIGURE 32.—Total-intensity anomalies of magnetic doublet of length, $l=1.5$ depth units.

TABLE 1.—Comparison of numerical values for two different definitions of β

l/d	0.01	0.10	0.50	1.00	1.50	2.00	5.00
β_1 -----	1.24	1.23	1.22	1.17	1.14	1.12	1.08
β_2 -----	2.52	2.68	2.79	3.00	3.19	3.21	3.59

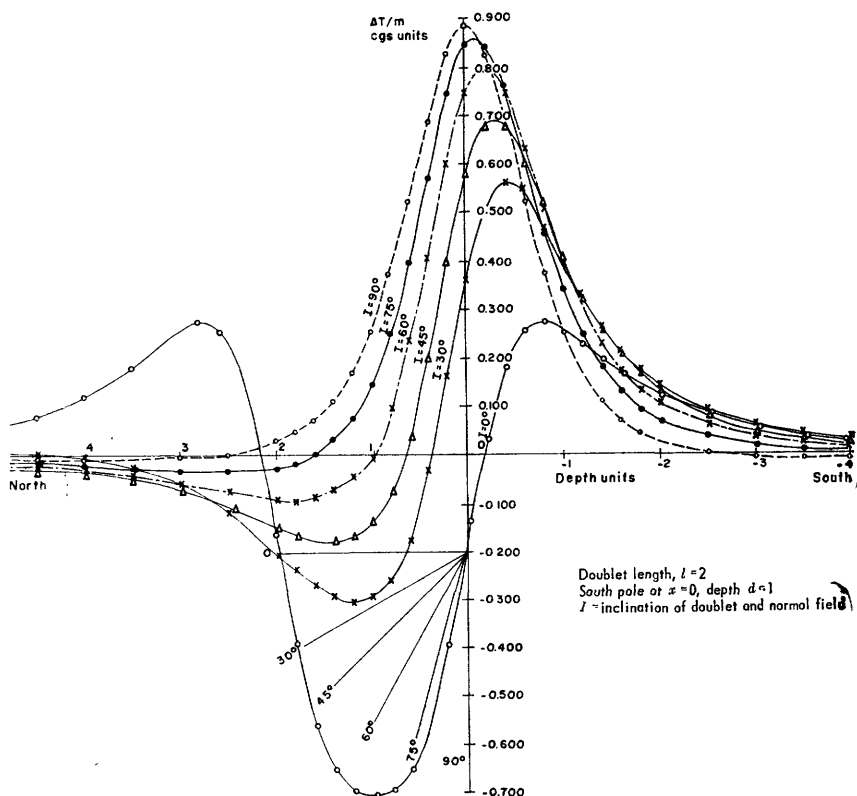
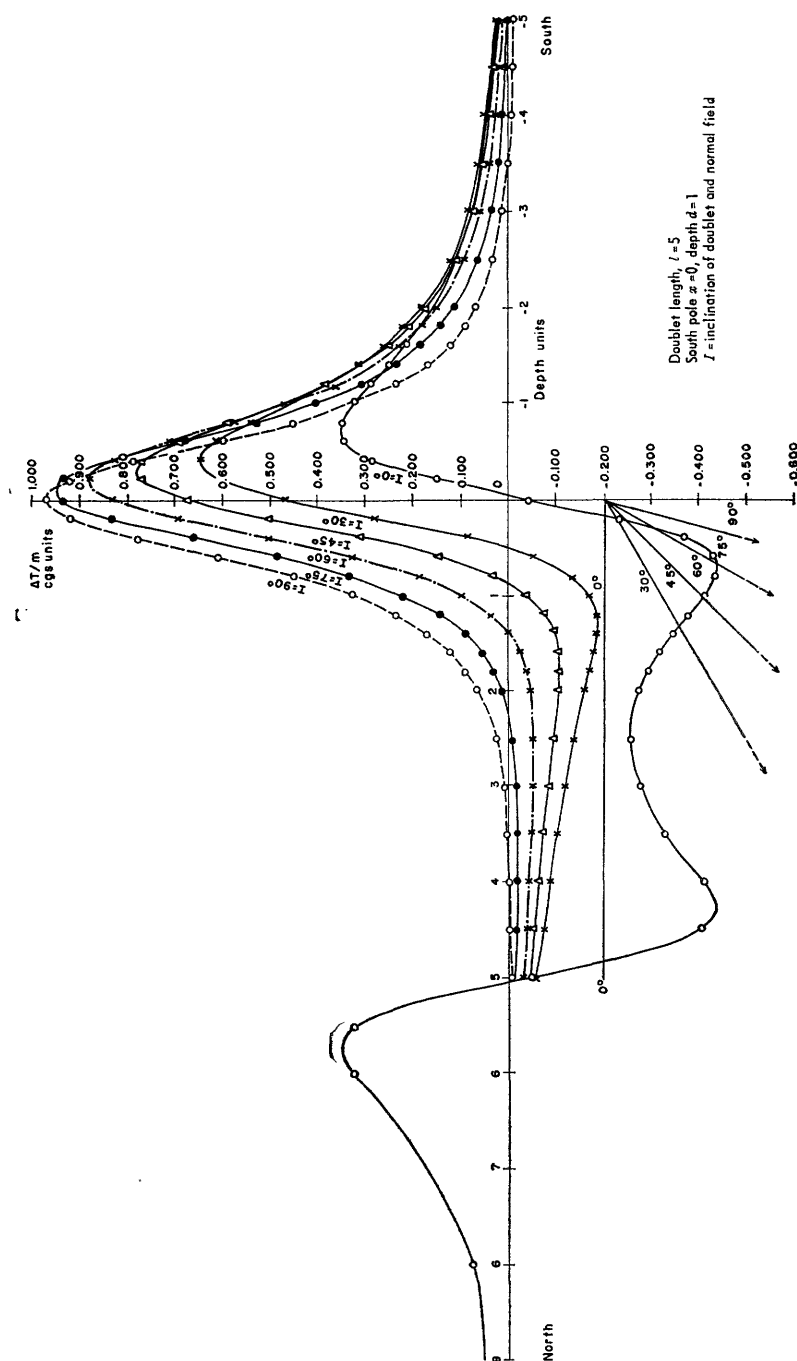


FIGURE 33.—Total-intensity anomalies of magnetic doublet of length, $l=2$ depth units.

The incremental changes in β_1 are too small to permit us adequately to distinguish among the different terms l/d , but those of β_2 are satisfactory for this purpose. If the choice were $\beta = (x_{\min} - x_{\max}) / (x_{\max} - x_{0.8})$, the increments in β would be larger, but this gain would be offset by uncertainties in the location of the minimum. Similar studies were made of families of theoretical $\Delta T(x)$ profiles for all the remaining inclinations. Abscissas yielding satisfactory values of β and δ are given in table 2, together with magnitudes of maximum and minimum values of $\Delta T(x)$ and their respective coordinates.

FIGURE 34.—Total-intensity anomalies of magnetic doublet of length, $l=5$ depth units.

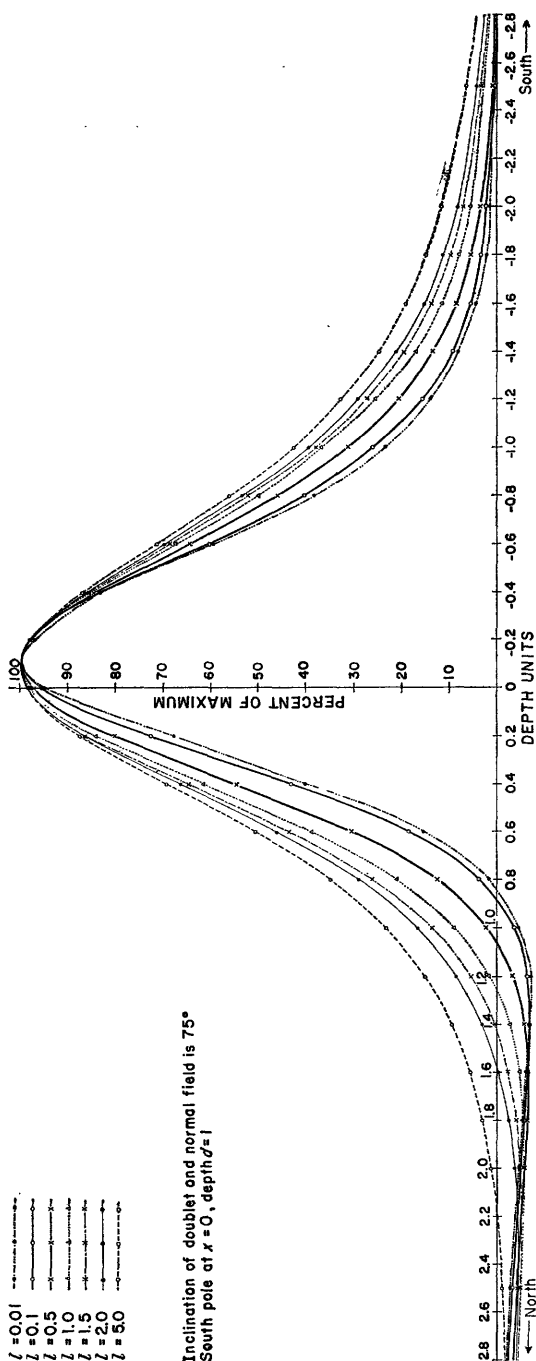
FIGURE 35.—Total-intensity anomalies of doublets showing effect of increasing length, l .

TABLE 2.—Parameters of magnetic doublets for inclinations, I , and length-to-depth ratios, l/d

[The positions $x_{0.1}$, $x_{0.2}$, $x_{0.3}$. . . indicate, respectively, abscissas of 10 percent, 20 percent, 30 percent . . . of the maximum value, ΔT_{\max} , of a given profile. Prime marks refer to more northerly abscissas. Upper pole is at $x=0$, $d=1$. Pole strength, $m=1$]

l/d	ΔT_{\max}	ΔT_{\min}	x_{\max}	x_{\min}	β	δ
Inclination 0°						
$[\beta = (x_{\min} - x_{\max}) / (x_{\min} - x_{0.5}), \quad \delta = x'_{0.5} - x_{0.5}]$						
0.01	0.002	-0.010	-1.20	0.01	3.16	0.78
.10	.020	-.098	-1.20	.05	3.20	.78
.50	.098	-.452	-1.00	.25	2.91	.83
1.00	.180	-.706	-.90	.50	2.80	1.02
1.50	.235	-.766	-.80	.75	2.46	1.28
2.00	.274	-.707	-.80	1.00	2.14	1.67
Inclination 30°						
$[\beta = (x_{\min} - x_{\max}) / (x_{\max} - x_{0.5}), \quad \delta = x'_{0.5} - x_{0.5}]$						
0.01	0.008	-0.008	-0.60	0.35	1.27	2.67
.10	.076	-.070	-.58	.43	1.31	2.77
.50	.290	-.252	-.53	.60	1.40	2.95
1.00	.440	-.347	-.46	.82	1.45	3.16
1.50	.516	-.332	-.43	1.02	1.61	3.39
2.00	.564	-.306	-.40	1.15	1.67	3.45
5.00	.649	-.185	-.35	1.32	1.72	3.90
Inclination 45°						
$[\beta = (x_{\min} - x_{\max}) / (x_{\max} - x_{0.5}), \quad \delta = x'_{0.5} - x_{0.5}]$						
0.01	0.013	-0.005	-0.40	0.58	1.60	1.71
.10	.111	-.046	-.35	.65	1.69	1.84
.50	.392	-.154	-.35	.85	2.00	1.94
1.00	.440	-.192	-.35	1.10	2.38	2.16
1.50	.638	-.192	-.35	1.30	2.66	2.30
2.00	.690	-.178	-.35	1.50	2.94	2.40
5.00	.780	-.104	-.35	1.80	3.77	2.66

TABLE 2.—Parameters of magnetic doublets for inclinations, I , and length-to-depth ratios, l/d —Continued

l/d	ΔT_{\max}	ΔT_{\min}	x_{\max}	x_{\min}	β	δ
Inclination 60°						
$[\beta = (x_{0.1} - x_{\max}) / (x_{\max} - x_{0.5}), \quad \delta = x'_{0.5} - x_{0.5}]$						
0. 01	0. 017	−0. 003	−0. 24	0. 85	1. 65	1. 05
0. 10	. 142	−. 026	−. 26	1. 00	2. 12	1. 06
0. 50	. 480	−. 081	−. 22	1. 20	2. 14	1. 19
1. 00	. 662	−. 098	−. 20	1. 40	2. 32	1. 29
1. 50	. 750	−. 096	−. 19	1. 68	2. 42	1. 36
2. 00	. 801	−. 089	−. 19	1. 80	2. 58	1. 40
5. 00	. 882	−. 050	−. 18	2. 50	2. 79	1. 48
Inclination 75°						
$[\beta = (x'_{0.1} - x_{\max}) / (x_{\max} - x_{0.5}), \quad \delta = x'_{0.5} - x_{0.5}]$						
0. 01	0. 018	−0. 001	−0. 12	1. 20	2. 52	1. 01
. 10	. 163	−. 011	−. 13	1. 40	2. 68	1. 05
. 50	. 540	−. 033	−. 11	1. 60	2. 79	1. 19
1. 00	. 730	−. 040	−. 10	2. 00	3. 00	1. 30
1. 50	. 817	−. 038	−. 10	2. 30	3. 19	1. 37
2. 00	. 865	−. 043	−. 09	2. 50	3. 21	1. 41
5. 00	. 950	−. 021	−. 09	3. 50	3. 59	1. 50
Inclination 90°						
$[\beta = x'_{0.05} - x_{0.5}, \quad \delta = x_{0.5}]$						
0. 01	0. 020	0. 000	0	1. 90	2. 22	0. 51
. 10	. 174	−. 003	0	2. 00	2. 25	. 52
. 50	. 556	−. 019	0	2. 50	2. 25	. 60
1. 00	. 750	−. 011	0	3. 00	2. 38	. 64
1. 50	. 840	−. 011	0	3. 50	2. 46	. 68
2. 00	. 889	−. 010	0	3. 50	2. 57	. 70
5. 00	. 938	−. 005	0	5. 70	2. 91	. 75

ANALYSIS OF ANOMALIES

To determine the magnetic-doublet equivalent of a suitable observed anomaly, a north-south profile is drawn through the maximum at any convenient scale. The zero datum line is drawn by inspection and is based on the mean undisturbed magnetic level. The magnetic inclination for the area is determined from isoclinal charts published by the U. S. Coast and Geodetic Survey (Deel and Howe, 1948) or from tables by Vestine and others (1947). The abscissas to be used in computing β are taken from table 2, for the inclination nearest to that observed. If the computed value of β falls within the range of those listed in the table, there is reason to believe that a doublet representation by the method described here is possible. Table 2 is entered for this value of β and a quantity l/d and a depth factor δ are determined by interpolation. The depth, d , to the near pole is calculated by dividing the corresponding horizontal distance on the observed profile by δ . The doublet length is then obtained from the product of d and l/d .

The calculation is best explained by an example. Consider the total-intensity profile over the inclined cylinder shown in figure 36, which was obtained from experiments on models. As the inclination

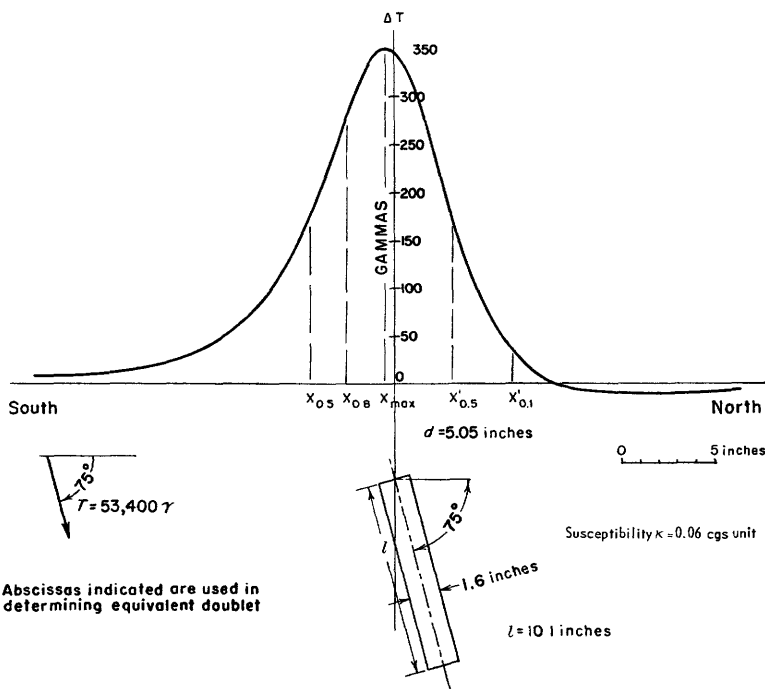


FIGURE 36.—Total-intensity anomaly of inclined cylinder; obtained from model experiment.

is 75° , the abscissas to be used in computing β and δ are x_{\max} , $x'_{0.1}$, $x_{0.5}$, $x'_{0.5}$ and $x_{0.8}$, as indicated by table 2. The maximum value of ΔT is 350γ ; therefore the x coordinates for 35γ , 175γ , 280γ , and 350γ are plotted as shown. Then $\beta = (x'_{0.1} - x_{\max}) / (x_{\max} - x_{0.8}) = 3.24$. Entering table 2 for $\beta = 3.24$ we obtain by interpolation an l/d of 2.2 and a δ of 1.42 inches. As $x'_{0.5} - x_{0.5} = 7.30$ inches on the profile, the depth is $d_e = (x'_{0.5} - x_{0.5}) / \delta = (7.30) / (1.42) = 5.1$ inches. The length is $l_e = (l/d)d_e = (2.2)(5.1) = 11.2$ inches. The depth and length are known to be $d_o = 5.05$ inches and $l_o = 10.1$ inches from model experiments. The results are unusually good even for a carefully controlled laboratory experiment.

OTHER USES OF COMPUTED ANOMALIES

Although figures 28 to 34 were computed primarily for determining the β and δ factors, they can be used for qualitative interpretations. For example, they provide information on the general shape of total-intensity anomalies to be expected from different rock masses magnetized by induction. When the horizontal dimensions of the mass are less than the depth to its top, a single doublet can be used to represent it. When the mass has a width less than the depth, but is extensive in the plane of the magnetic meridian, the anomalies of several doublets alined in parallel in the meridian can be combined to give an equivalent anomaly. This simple addition of two or more anomalies is permissible by the superposition law of potential theory.

The following generalizations based on figures 28 to 35 are helpful in interpretations:

1. The anomaly of the vertical doublet is symmetric with respect to the axis.
2. For inclined doublets, the maximum of an anomaly is always south of the upper pole, and the amount of the south shift increases with decrease in the inclination.
3. For a given depth and doublet length, a decrease in the inclination diminishes the amplitude of the maximum and increases that of the minimum. The effect on the steepest gradients is practically negligible, and the north slopes of the profile remain parallel for all inclinations. The latter fact suggests that fitting a slope is meaningless, because the diagnostic characteristics of the anomaly are involved in the south slope and minimum as well.
4. If other parameters are equal, an increase in doublet length decreases the steepest gradients of the anomaly, as can be seen explicitly in figure 25.
5. For an inclination $I=0$, a double minimum develops when l is about three times the depth, which indicates resolution of the effects of the two poles.

6. For l very large, the theory reduces to that of a point pole, which we have already treated (Henderson and Zietz, 1948).

MAGNETIC MODEL EXPERIMENTS

To investigate the method of study when applied to fields produced by physically realizable bodies, a series of experiments on magnetic models was carried out. Facilities of the Naval Ordnance Laboratory at White Oak, Md., were made available for these and other tests. A detailed account of the experiments is contained in a preliminary report by Zietz and Henderson (1956).

The experimental set up is an elaborate modification of that used by Alldredge and Dichtel (1949) in their interpretation of the Bikini magnetic data. Three large mutually perpendicular Helmholtz-type coils on 30-foot frames are individually energized by an adjustable d-c voltage supply. In this way, the magnitude and direction of the uniform field of the earth can be simulated over a relatively large volume about the center of the system. A model is placed at the center and the anomaly field produced by the induced magnetism of the model is measured by means of a flux-gate magnetic detector of fixed orientation on a tower having powered vertical positioning. The detector tower is mounted on a carriage which moves in an east-west or a north-south direction. Continuous registration of data is accomplished with a null-type recorder. Once the model has been set up and the detector oriented in the direction of the simulated field, all operations are conveniently effected from control panels mounted in a console. The accuracy of the magnetometer system is $\pm 3 \gamma$.

The models were prepared from a mixture of gypsum plaster and powdered magnetite in the ratio of 2:1 by volume. For this study, the models were primarily cylinders; however, a few double-layer models 0.5 inch thick were also used. All remanent magnetism in the models was carefully removed by electrical "shaking" in a zero ambient field. The cylinders and the detector were aligned codirectionally with the field at the center of the Helmholtz system. The applied total field was invariably 53,400 γ .

TESTS ON CYLINDRICAL MODELS

A profile of a typical ΔT anomaly over a cylinder is shown in figure 36 together with data for computation. Similar profiles for 5 cylinders in fields of inclinations $I=0^\circ$, 75° , and 90° were also analyzed and the results are given in table 3. The measured length of the cylinder and depth to the center of the base nearer the origin are in columns headed " l_o " and " d_o " and the corresponding computed lengths and

depths are in columns " l_c " and " d_c ." In general the calculated depths are in better agreement with those measured than are the calculated lengths.

TABLE 3.—Comparison of calculated doublet lengths and depths with those used in model experiments

[Dip of cylinders equal to inclination of impressed field. Linear dimensions in inches]

Inclination	Cylinder No.	Diameter	Observed values			Computed values		
			l_o	d_o	$(l/d)_o$	$(l/d)_c$	l_c	d_c
0°	I	2.15	5.00	4.90	1.02	1.3	5.5	4.2
		2.15	5.00	6.80	.74	1.0	5.8	5.8
		2.15	5.00	8.50	.59	1.1	7.7	7.0
	II	1.00	5.10	3.70	1.38	1.8	5.4	3.0
		1.00	5.10	5.75	.89	1.8	7.7	4.4
	III	4.05	10.00	9.00	1.11	1.5	11.2	7.5
		4.05	10.00	14.20	.70	1.2	14.8	12.3
	IV	1.60	10.10	6.45	1.57	1.8	10.8	6.2
		1.60	10.10	11.50	.88	1.8	15.1	8.4
	V	1.50	18.00	5.85	3.08	3.8	17.1	4.5
		1.50	18.00	7.35	2.45	2.9	21.5	7.4
30°	I	2.15	5.00	3.75	1.33	1.2	5.2	4.3
		2.15	5.00	5.65	.88	1.1	7.4	7.0
	II	1.00	5.10	3.15	1.62	1.2	4.2	3.5
		4.05	10.00	5.00	2.00	1.2	9.5	7.9
	IV	1.60	10.10	5.70	1.77	.8	6.4	7.7
		1.50	18.00	4.92	3.66	3.5	20.7	5.9
75°	I	2.15	5.00	5.00	1.00	.9	4.9	5.3
		2.15	5.00	6.65	.75	1.4	9.1	6.4
	III	4.05	10.00	5.00	2.00	2.6	14.6	5.6
		1.60	10.10	5.05	2.00	2.2	11.1	5.1
	IV	1.60	10.10	10.10	1.00	1.1	11.1	10.0
		1.50	18.00	4.50	4.00	5.7	25.6	4.5
90°	I	2.15	5.00	4.50	1.11	1.8	7.9	4.5
		1.00	5.10	4.60	1.11	1.5	6.6	4.4
	III	4.05	10.10	5.00	2.02	2.6	14.6	5.6
		4.05	10.10	10.00	1.01	1.5	15.0	10.0
	V	1.50	18.00	4.00	4.50	5.0	21.5	4.3
		5.85	9.90	5.05	1.96	1.2	7.8	6.5

Comparisons of columns $(l/d)_o$ and $(l/d)_c$ also afford some idea of the accuracy involved. Calculations of doublet length are more reliable for low magnetic inclinations than for high inclinations. In low inclinations the more remote source is nearer the surface and can therefore have a greater expression in the data.

Uncertainties in the location of apparent poles of a cylindrical body impose limitations on the extent to which comparisons of observed and computed values of l and d can be made. Theoretically, at least, it is expected that d_c will be greater than d_o and l_c will be less than l_o , because the apparent poles must lie within the body. In this particular investigation, the errors developed in the process rendered indiscernible any such systematic trends.

For a given cylinder the errors in computed lengths and depths increase as l/d decreases, which is to be expected. The depth d_c in table 3 was computed with a mean error of 14 percent; the l_c was computed with a mean error of 29 percent.

MAGNETIC DOUBLE-LAYER MODELS

The method was applied to anomaly fields measured over models consisting of plaster-magnetite horizontal slabs 0.5 inch thick and of different rectangular dimensions. The 5 inches \times 5 inches model at a depth of 5 inches gave fair results, as shown in table 4. Here, the doublet length, l , is logically the slant distance in inches (see inset, fig. 37) measured along the direction of the field between the upper and lower faces, and is given by $l_o = 5/\cos I$ for $0 \leq I \leq 0.032\pi$ and $l_o = 0.5 \text{ inch} \sin I$ for $0.032\pi \leq I \leq \pi/2$. The computed l_o , although not entirely satisfactory for determining the thickness, does in a general way decrease with increasing I and gives the order of magnitude. The results suggest that the calculation of depth to the top surface is more

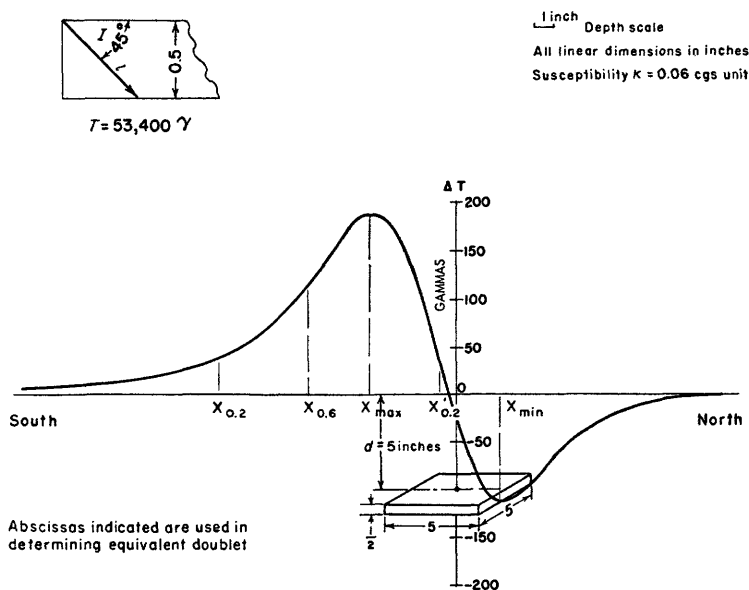


FIGURE 37.—Total-intensity anomaly of magnetized plate; obtained from model experiment.

accurate at low magnetic inclinations. When applied to double-layer models of larger horizontal dimensions, for example, 0.5 inch \times 10 inches \times 10 inches, the method failed, because the β values fell outside the range of table 2. For models 0.5 inch thick but of plan less than 5 inches \times 5 inches, the method would very likely be successful.

TABLE 4.—*Application of magnetic-doublet theory to field of horizontal slab*

[Fields obtained from laboratory measurements on body of dimensions 0.5 in. \times 5 in. \times 5 in. at a depth of 5 in. Linear dimensions in inches]

Inclination ¹	Model	$(l/d)_o$	$(l/d)_o$	l_o	d_o
0°	5.00	1.00	1.12	5.5	4.9
30°	1.00	.20	.60	3.3	5.0
45°	.85	.17	.56	3.2	5.8
60°	.58	.11	.10	.6	6.3
75°	.52	.10	.20	1.2	6.2

¹ Observations over the center line at $I=90^\circ$ were not made.

Some idea of the limits of the size of bodies that can be analyzed in this manner can be gained from the following expression for the ΔZ anomaly on the axis of a vertical cylinder in a vertical field:

$$\Delta Z(0) = 2\pi\kappa Z_o \{ (d+l)/[(d+l)^2 + \rho^2]^{\frac{1}{2}} - d/(d^2 + \rho^2)^{\frac{1}{2}} \} \quad (2)$$

where Z_o is the impressed vertical intensity field, ρ the radius, d the depth to the upper base, and κ the susceptibility. If the expression (2) is expanded in a binomial series the result is

$$\Delta Z(0) = 2\pi\kappa Z_o \{ (\frac{1}{2})[\rho^2/d^2 - \rho^2/(d+l)^2] - \frac{3}{8}[\rho^4/d^4 - \rho^4/(d+l)^4] + \dots \} \quad (3)$$

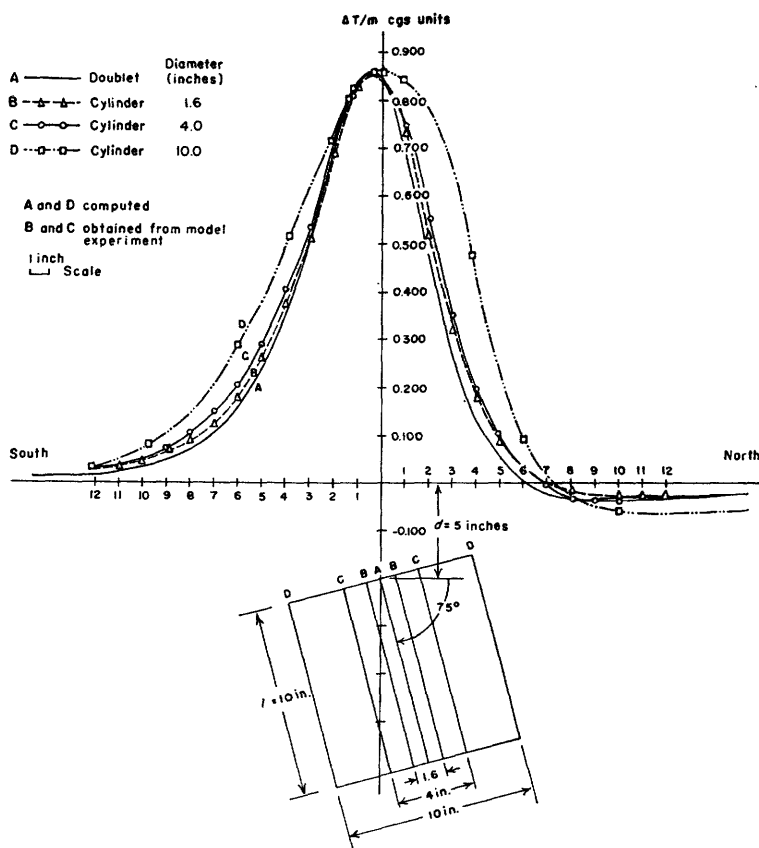
which is valid for $\rho < d$. For $\rho \ll d$ only the first term is significant and (3) may be written

$$(\text{cylinder}) \quad \Delta Z(0) \approx \pi\kappa Z_o \rho^2 [1/d^2 - 1/(d+l)^2]. \quad (4)$$

The expression (4) has the same geometrical form as the formula for a vertical doublet in a vertical field:

$$\Delta Z(0) = m [1/d^2 - 1/(d+l)^2]. \quad (5)$$

Although (4) and (5) are meaningful only at the origin, and although l for the cylinder is not identical with l for the doublet, the comparison nevertheless suggests that the mean radius of a body must be less than its depth of burial if it is to be successfully represented as a magnetic doublet. The experiment above on the 5 inches \times 5 inches body at a depth of 5 inches, with an effective radius $\rho = 5/\sqrt{\pi}$ confirms



MAXIMUMS HAVE BEEN ADJUSTED TO DOUBLET WITH $\Delta T_m = 0.865$ cgs units

FIGURE 38.—Anomalies of inclined cylinders showing effect of increasing diameter.

this result. In the 10 inches \times 10 inches body at the same depth, the effective radius is $\rho = 10/\sqrt{\pi}$ and failure is to be expected.

To investigate further the effect of the radius on doublet representation, the anomalies of 3 coaxial cylinders 10 inches long in a field of inclination 75° were adjusted so that the ΔT_{\max} of each was equal to that of a doublet of the same length, as shown in figure 38. For all, the depth to the center of the top is d and the length $2d$. The radii of cylinders B, C, and D are $\rho = 0.16d$, $0.4d$, and d . The anomalies of B and C were obtained from model experiments. The doublet anomaly was computed from formula (1). The anomaly for cylinder D was computed numerically by means of a modification

(Henderson, R. G., and Zietz, Isidore, 1958) of Gassman's three-dimensional integration process (Gassman 1951). The latter was checked by application to cylinder C whose anomaly it reproduced faithfully. In figure 38, it is quite clear that the shape of the anomaly does not alter radically from that of a doublet as the radius increases to 0.4 depth. When the radius equals the depth, the shape of the anomaly bears little resemblance to that of a doublet; therefore the doublet-analysis method cannot be used. It also appears from figure 38 that the possibility of determining the radius of a cylinder from a dipolelike anomaly is very remote. A rigorous investigation of this matter is not possible because of the lack of a closed form for calculating the ΔT anomaly of a cylinder.

PRACTICAL APPLICATIONS

Aeromagnetic observations over geologic bodies of known depth, dimensions, and magnetic properties were not available for testing. The method was therefore applied to the surveys in areas for which we have some knowledge, although fragmentary, of the depth to crystalline magnetic rocks. If the rocks are exposed, the problem is simply to determine from magnetic data the altitude of the surveying airplane above the surface. In other areas where the crystalline rocks are buried, the "known" depths can be inferred from drilling data or from geologic information. Although calculations of l were made, the results are not included here because depth-extent data for purposes of comparison were nonexistent.

The anomalies to which we have applied this method are shown in figures 39 to 43. The line $A-A'$ in each figure indicates the profile across the anomaly, and $B-B'$ indicates the horizontal distance used with the appropriate δ in the depth calculation. The values of β are not shown for these applications.

SOUTHEAST MISSOURI

On the U. S. Geological Survey aeromagnetic map of the Coldwater quadrangle, in southeastern Missouri (fig. 39), there are several anomalies over exposed felsite, particularly where the felsite is in contact with granite. Calculations of the depth of the source were made on the closed magnetic high about 1 mile west of Cedar Mountain in the Coldwater quadrangle and a depth of 870 feet was obtained. As the elevation of the airplane above the surface was 800 feet, the calculated value is regarded as satisfactory.

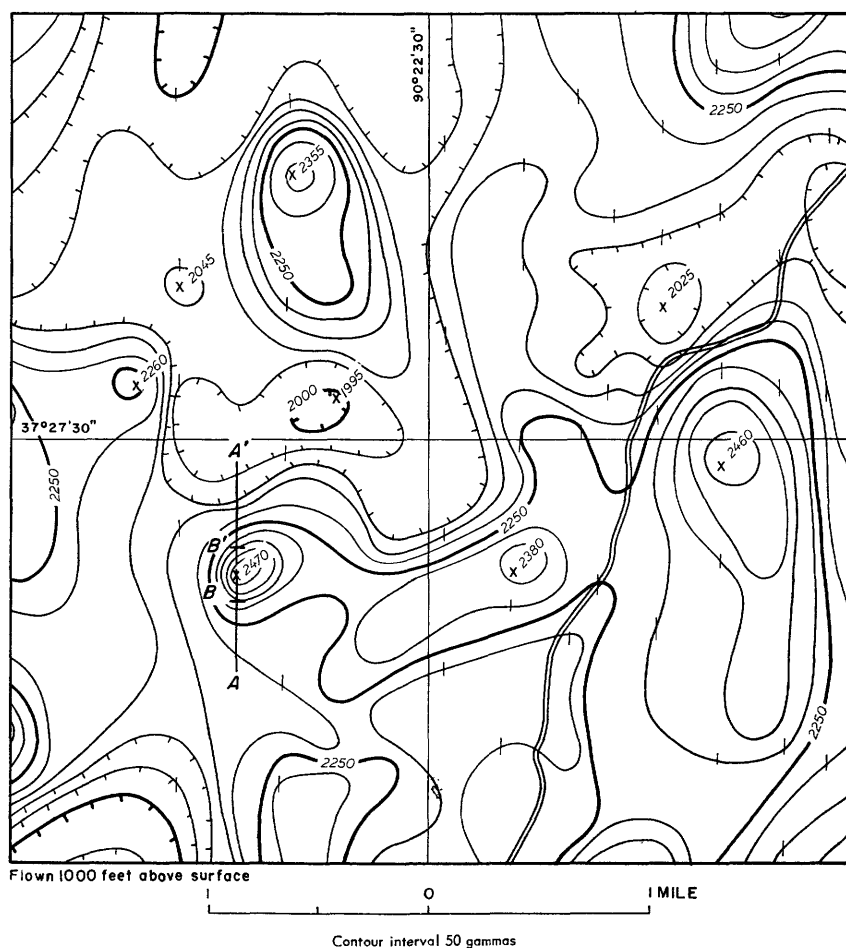


FIGURE 39.—Total-intensity aeromagnetic map of part of Coldwater quadrangle, Missouri.

INDIANA

The anomaly near Bryant in T. 24 N., R. 14 E., in Jay County, Ind. (fig. 40), was analyzed by the doublet method and a depth to magnetic rocks of 5,400 feet below the aircraft was found. On the basis of a well in sec. 9, T. 24 N., R. 13 E., Precambrian igneous rocks in the area are estimated to be at a depth of 3,350 feet, or 4,350 feet below the level of observations.

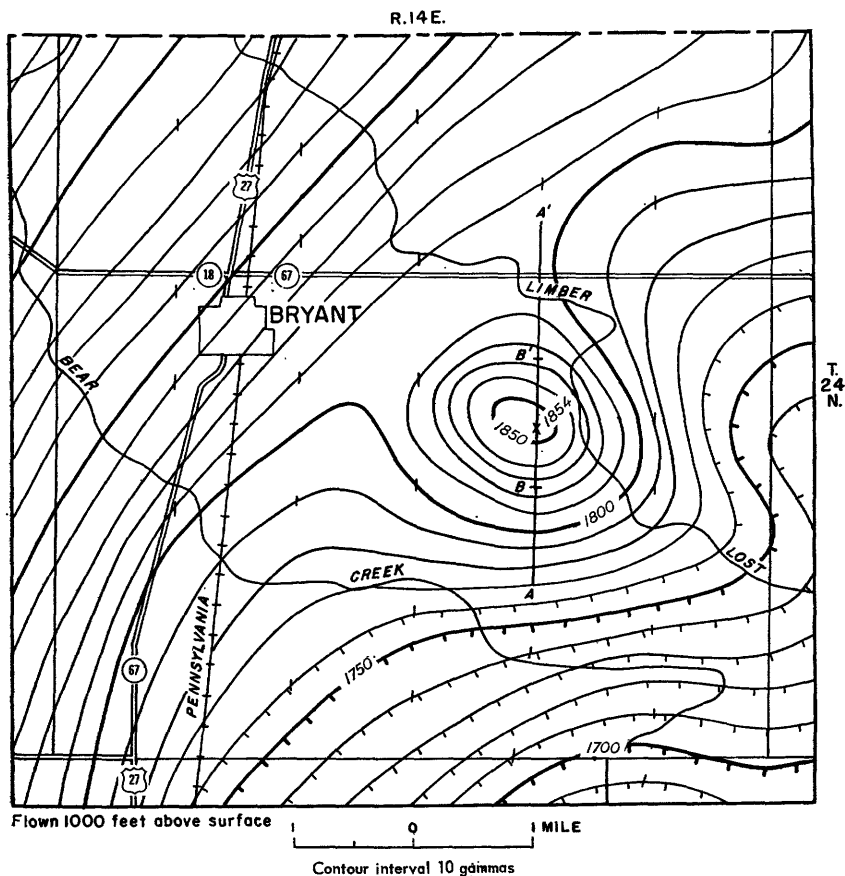
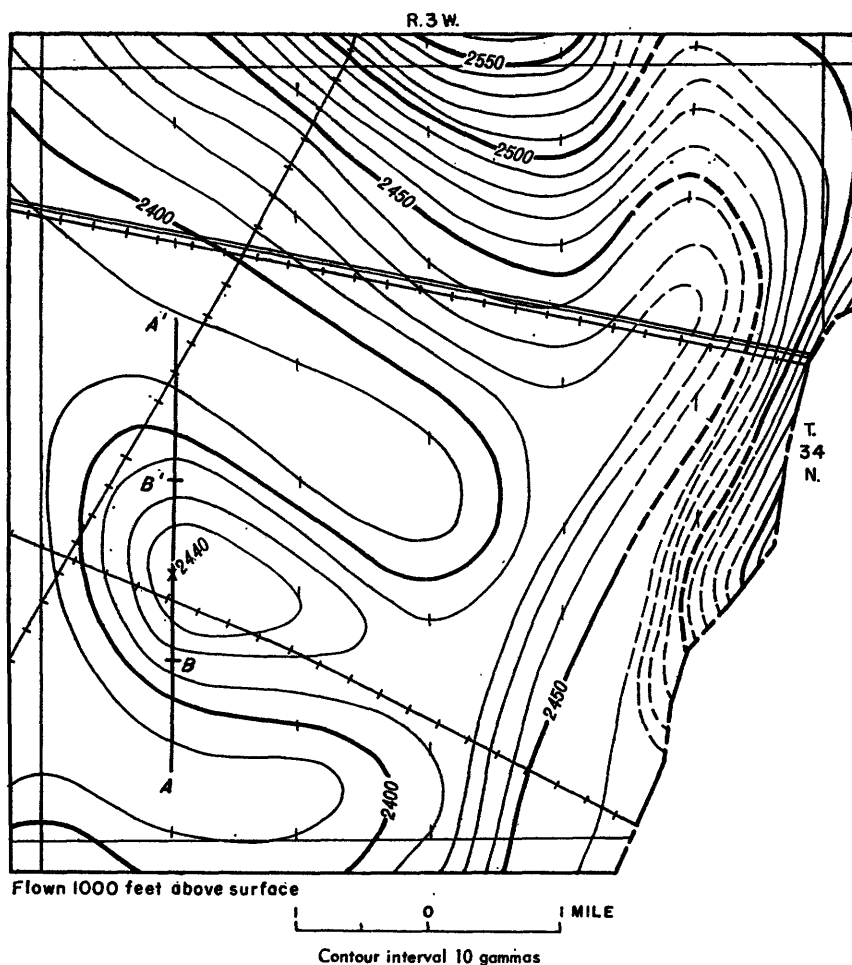


FIGURE 40.—Total-intensity aeromagnetic map of area near Bryant, Jay County, Ind.

In La Porte County, Ind. (fig. 41), information on depth to igneous rocks is scanty, as the nearest wells are about 50 miles away. Geologists estimate the depth to the Precambrian is 6,200 feet at the location of the anomaly 6 miles northeast of La Crosse, in T. 34 N., R. 3 W. The depth calculated by doublet analysis is 6,900 feet below the airplane.

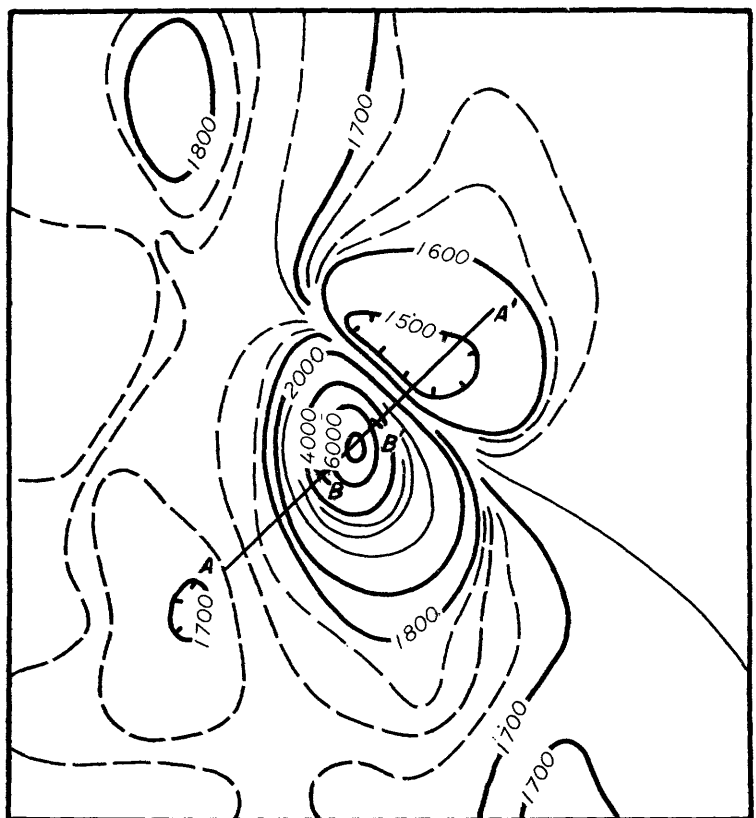


$B-B'$ IS HALF-MAXIMUM DISTANCE ON PROFILE $A-A'$

FIGURE 41.—Total-intensity aeromagnetic map of T. 34 N., R. 3 W., La Porte County, Ind.

ONTARIO, CANADA

A prominent magnetic anomaly about 1 mile southeast of Marmora, Ontario, appears on the Campbellsford aeromagnetic map (Canada Geological Survey [1950]). Drilling information indicates there are 90 to 150 feet of limestone of Paleozoic age overlying iron-bearing Precambrian rocks in the area. The disturbing rocks are known to contain magnetite. A calculation on the northeasterly profile ($A-A'$ in fig. 42) gave a depth of 850 feet below the airplane in comparison with probable depths of 600 to 650 feet.



Flown 500 feet
above sea level

Canada Geological
Survey

0 1 MILE

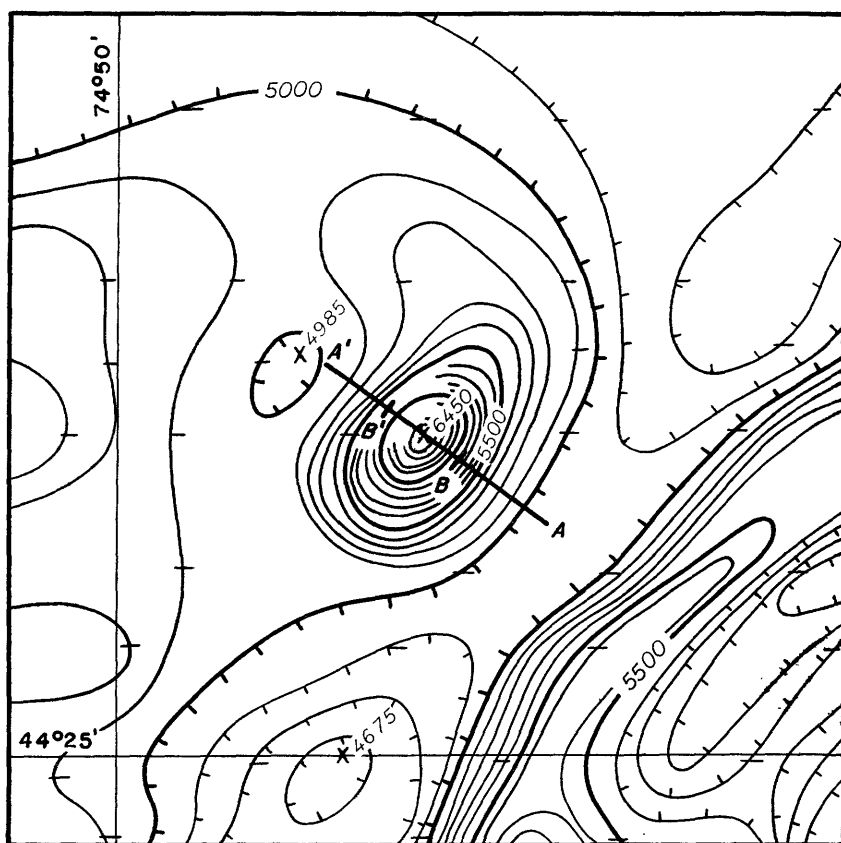
Contour intervals 25, 100, 200, 500, and 2,000 gammas

$B-B'$ IS HALF-MAXIMUM DISTANCE ON PROFILE $A-A'$

FIGURE 42.—Total-intensity aeromagnetic map of area near Marmora, Ontario, Canada.

ADIRONDACK MOUNTAINS, N. Y.

Analysis of the isolated magnetic anomaly in the north-central part of the Stark quadrangle in the Adirondack Mountains, (fig. 43) indicated a depth of 1,050 feet for the source. The airplane was 1,000 feet above the ground. The rocks in the area have been mapped as hornblende granite with a few layers of metasediment. It is very likely that the disturbing rocks are near the surface.



Flown 1000 feet
above surface

0 1 MILE

Contour interval 100 gammas

B-B' IS HALF-MAXIMUM DISTANCE ON PROFILE *A-A'*

FIGURE 43.—Total-intensity aeromagnetic map of northern part of Stark quadrangle, New York;

CONCLUSIONS

The application of magnetic-doublet theory has been shown to be reasonably effective for determinations of the depth of cylindrical laboratory models oriented in the direction of the earth's magnetic field. The determination of doublet length is less reliable. In general the method yields better results for bodies in low magnetic inclinations. The method cannot be expected to give satisfactory values in high magnetic inclinations when the mean radius of a horizontal section exceeds the depth of burial. The most practical use of the method is in depth determinations. The anomaly curves of figures 28 to 34 are also useful qualitatively in obtaining some idea of the anomalies to be expected at various inclinations and the relative displacement of maximums.

LITERATURE CITED

- Aldredge, L. R., and Dichtel, W. J., 1949, Interpretation of Bikini magnetic data: *Am. Geophys. Union Trans.*, v. 30, p. 831-385.
- Balsley, J. R., and others, 1954, Total aeromagnetic intensity and geologic map of Stark, Childwold, and part of Russell quadrangles, New York: U. S. Geol. Survey Geophys. Inv. Map GP 117, scale 1 inch=about 1 mile [1955].
- Canada Geological Survey [1950], Aeromagnetic map, Campbellford sheet [Ontario] No. 315: Canada Geol. Survey Geophysics Paper 13, scale 1 inch=1 mile.
- Deel, S. A., and Howe, H. H., 1948, United States magnetic tables and magnetic charts for 1945: U. S. Coast and Geod. Survey Serial 667, 137 p.
- Dempsey, W. J., and Duffner, R. T., 1949, Total intensity aeromagnetic map of Coldwater quadrangle [Madison and Wayne Counties] Missouri: U. S. Geol. Survey Geophys. Inv. Map, scale 1 inch= $\frac{1}{2}$ mile.
- Dempsey, W. J., Henderson, J. R., and Duffner, R. T., 1949, Total intensity aeromagnetic map of La Porte County, Indiana: U. S. Geol. Survey Geophys. Inv. Map, scale 1 inch=1 mile.
- Gassman, Fritz, 1951, Graphical evaluation of the anomalies of gravity and of the magnetic field, caused by three-dimensional bodies: 3d World Petroleum Cong., The Hague 1951, Proc., sec., 1, p. 613-621.
- Heiland, C. A., 1940, Geophysical exploration: New York, Prentice-Hall Inc., 1013 p.
- Henderson, J. R., and Meuschke, J. L., 1951, Total intensity aeromagnetic map of Jay County, Indiana: U. S. Geol. Survey Geophys. Inv. Map GP 86, scale 1 inch=1 mile.
- Henderson, J. R., Jr., and Zietz, Isidore, 1958, Interpretation of an aeromagnetic survey in Indiana: U. S. Geol. Survey Prof. Paper 316-B [in press].
- Henderson, R. G., and Zietz, Isidore, 1948, Analysis of total magnetic intensity anomalies produced by point and line sources: *Geophysics*, v. 13, p. 428-436.
- 1957, Graphical calculation of total-intensity anomalies of three-dimensional bodies: *Geophysics*, v. 22, p. 887-904.

- Jakosky, J. J., 1950, *Exploration geophysics*: Los Angeles, Calif., Trija Publishing Co., 1195 p.
- Nettleton, L. L., 1940, *Geophysical prospecting for oil*: New York, McGraw-Hill Book Co., 444 p.
- Vacquier, Victor, Steenland, N. C., Henderson, R. G., and Zietz, Isidore, 1951, Interpretation of aeromagnetic maps: *Geol. Soc. America Mem.* 47, 151 p.
- Vestine, E. H., and Davids, Norman, 1945, Analysis and interpretation of geomagnetic anomalies: *Terrestrial Magnetism and Atmospheric Electricity*, v. 50, p. 1-36.
- Vestine, E. H., Laport, Lucile, Lange, Isabelle, Cooper, Caroline, and Hendrix, W. C., 1947, Description of the earth's main magnetic field and its secular change, 1905-1945: *Carnegie Inst. Washington Pub.* 578, 532 p.
- Zietz, Isidore, and Henderson, R. G., 1956, A preliminary report on model studies of magnetic anomalies of three-dimensional bodies: *Geophysics*, v. 21, p. 794-814.

the 1990s, the number of people in the world who are undernourished has increased from 600 million to 800 million (FAO 1996).

There are a number of reasons why the world's population is becoming more undernourished. First, the world's population is growing rapidly, and the number of mouths to feed is increasing. Second, the world's population is becoming more urbanized, and the demand for food is increasing. Third, the world's population is becoming more affluent, and the demand for food is increasing.

There are a number of ways in which the world's population can be fed. First, the world's population can be fed by increasing the production of food. Second, the world's population can be fed by increasing the efficiency of food production. Third, the world's population can be fed by increasing the distribution of food.

There are a number of ways in which the world's population can be fed. First, the world's population can be fed by increasing the production of food. Second, the world's population can be fed by increasing the efficiency of food production. Third, the world's population can be fed by increasing the distribution of food.

There are a number of ways in which the world's population can be fed. First, the world's population can be fed by increasing the production of food. Second, the world's population can be fed by increasing the efficiency of food production. Third, the world's population can be fed by increasing the distribution of food.

There are a number of ways in which the world's population can be fed. First, the world's population can be fed by increasing the production of food. Second, the world's population can be fed by increasing the efficiency of food production. Third, the world's population can be fed by increasing the distribution of food.

There are a number of ways in which the world's population can be fed. First, the world's population can be fed by increasing the production of food. Second, the world's population can be fed by increasing the efficiency of food production. Third, the world's population can be fed by increasing the distribution of food.

There are a number of ways in which the world's population can be fed. First, the world's population can be fed by increasing the production of food. Second, the world's population can be fed by increasing the efficiency of food production. Third, the world's population can be fed by increasing the distribution of food.

There are a number of ways in which the world's population can be fed. First, the world's population can be fed by increasing the production of food. Second, the world's population can be fed by increasing the efficiency of food production. Third, the world's population can be fed by increasing the distribution of food.

There are a number of ways in which the world's population can be fed. First, the world's population can be fed by increasing the production of food. Second, the world's population can be fed by increasing the efficiency of food production. Third, the world's population can be fed by increasing the distribution of food.

the 1990s, the number of people in the UK who are aged 65 and over has increased from 10.5 million to 12.5 million, and the number of people aged 75 and over from 4.5 million to 6.5 million (Office of National Statistics 1999).

There is a growing awareness of the need to address the needs of older people in the community. The Department of Health (1999) has published a strategy for older people, which sets out a vision for the future of older people's services. The strategy is based on the principle of 'active ageing', which is the process of maintaining and enhancing the health, participation and security of older people. The strategy also sets out a number of key objectives, including: to improve the health and well-being of older people; to increase the participation of older people in society; and to ensure that older people are able to live in their own homes and communities for as long as possible.

The strategy also sets out a number of key actions, including: to improve the health and well-being of older people; to increase the participation of older people in society; and to ensure that older people are able to live in their own homes and communities for as long as possible. The strategy also sets out a number of key actions, including: to improve the health and well-being of older people; to increase the participation of older people in society; and to ensure that older people are able to live in their own homes and communities for as long as possible.

The strategy also sets out a number of key actions, including: to improve the health and well-being of older people; to increase the participation of older people in society; and to ensure that older people are able to live in their own homes and communities for as long as possible. The strategy also sets out a number of key actions, including: to improve the health and well-being of older people; to increase the participation of older people in society; and to ensure that older people are able to live in their own homes and communities for as long as possible.

The strategy also sets out a number of key actions, including: to improve the health and well-being of older people; to increase the participation of older people in society; and to ensure that older people are able to live in their own homes and communities for as long as possible. The strategy also sets out a number of key actions, including: to improve the health and well-being of older people; to increase the participation of older people in society; and to ensure that older people are able to live in their own homes and communities for as long as possible.

The strategy also sets out a number of key actions, including: to improve the health and well-being of older people; to increase the participation of older people in society; and to ensure that older people are able to live in their own homes and communities for as long as possible. The strategy also sets out a number of key actions, including: to improve the health and well-being of older people; to increase the participation of older people in society; and to ensure that older people are able to live in their own homes and communities for as long as possible.

The strategy also sets out a number of key actions, including: to improve the health and well-being of older people; to increase the participation of older people in society; and to ensure that older people are able to live in their own homes and communities for as long as possible. The strategy also sets out a number of key actions, including: to improve the health and well-being of older people; to increase the participation of older people in society; and to ensure that older people are able to live in their own homes and communities for as long as possible.

The strategy also sets out a number of key actions, including: to improve the health and well-being of older people; to increase the participation of older people in society; and to ensure that older people are able to live in their own homes and communities for as long as possible. The strategy also sets out a number of key actions, including: to improve the health and well-being of older people; to increase the participation of older people in society; and to ensure that older people are able to live in their own homes and communities for as long as possible.